Chemical Engineering Journal 163 (2010) 219–229

Contents lists available at ScienceDirect

Chemical Engineering Journal

journal homepage: www.elsevier.com/locate/cej

Thick film titania on glass supports for vapour phase photocatalytic degradation of toluene, acetone, and ethanol

Nageswara Rao Neti[a,*], Geeta Rani Parmar[a], Snejana Bakardjieva[b], Jan Subrt[b]

[a] National Environmental Engineering Research Institute, Nehru Marg, Nagpur 440020, India
[b] Institute of Inorganic Chemistry of the ASCR, v.v.i., 250 68 Rez, Czech Republic

ARTICLE INFO

Article history:
Received 4 March 2010
Received in revised form 21 June 2010
Accepted 19 July 2010

Keywords:
Titania photocatalyst
Thick films
Glass support
Volatile organic compounds
Photodegradation

ABSTRACT

Thick film titania photocatalysts (50–100 μm, Degussa P-25 TiO_2) coated on two types of soda glass supports viz. beads (TiO_2/B) and Rasching rings (TiO_2/R) were tested in vapour phase photodegradation of toluene (63–383 g m^{-3}), acetone (116–1161 g m^{-3}), and ethanol (116–1161 g m^{-3}) in a batch recirculation photoreactor at 60–70 °C. The concentrations of the substrates were 10- to 100-fold higher than those reported previously in similar investigations. The films were characterized by using SEM for morphology and EDX for elemental composition and mapping. Further, the effects of water vapour and shape and packing of the glass supports on the photodegradation kinetics were examined. The TiO_2 films on both the glass supports demonstrated high activity for photodegradation of toluene, acetone, and ethanol according to first-order kinetics. The apparent rate constants (k_a) were found to vary from 1.48×10^{-2} to 9.4×10^{-3} g m^{-3} min^{-1} for the photodegradation of toluene on both TiO_2/B and TiO_2/R; 5.57×10^{-2} to 1.29×10^{-2} g m^{-3} min^{-1} for TiO_2/B and 6.70×10^{-2} to 1.17×10^{-2} g m^{-3} min^{-1} for TiO_2/R for acetone; and 2.14×10^{-1} to 1.96×10^{-2} g m^{-3} min^{-1} and 7.25×10^{-2} to 3.51×10^{-2} g m^{-3} min^{-1} using TiO_2/R for ethanol photodegradation. The efficient photodegradation of higher concentration of toluene, acetone, and ethanol was attributed to (i) availability of more amounts of active sites on the thick TiO_2 films for adsorption of VOCs, (ii) their photodegradation within 'photoactive zone' constituting outer surface layer of thick TiO_2 coating and (iii) higher reactor temperature. The SEM and EDX data suggest migration of sodium ions across glass/TiO_2 interface into 'photoactive zone' of the thick TiO_2 layers did not occur. The TiO_2/R appear to show better efficiency in comparison with TiO_2/B because their packing in the reactor allows for better illumination of catalysts surface.

1. Introduction

Heterogeneous photocatalysis (TiO_2/UV) for oxidative removal of organic pollutants from contaminated air and water has become increasingly relevant in environmental remediation because of its efficiency and broad applicability [1–7]. The photocatalytic oxidation of many volatile organic compounds (VOCs) has been reported [8–12]. For example, toluene [13–21], acetone [22,12,23–26], TCE [13,27], ethanol [28–31,15,32], acetaldehyde [15,33,34], formaldehyde [35], methyl tertiary butyl ether [36], were successfully degraded using TiO_2/UV technique.

Literature survey revealed that most of the previous studies explored VOC concentration in the range 0.05–15 g m^{-3}. Moreover, the titania catalyst was applied as a coating on glass and other support materials [34–38], reactor tubes, glass micro-fibre filter, Al sheet, porous Vycor glass support, glass rings, cylinders and tubes of different diameter. Very thin films of TiO_2, often a few tens of nanometer, were applied. The TiO_2/supports were calcined at high temperatures (i.e., 350–700 °C) to improve crystallinity of oxide layer as well as its adhesion to support [41]; but this also caused decrease in photoactivity due to migration of Na ions from soda glass into TiO_2 layer [34–37] and also foreign metal ions (Cr, Mn, and Fe) from stainless steel support [41]. A fixed bed type of photocatalyst in a flow-through reactor was generally used for the degradation of air-bound VOCs in a batch recirculation mode. However, the influence of the shape and density of the glass supports that reflect on packing density and hence weight of the photoreactor were explored rarely. Further, the effect of calcining TiO_2/glass supports at a lower temperature, especially when previously made titania powder is used, and photodegradation rates at 10–100 times greater concentration of the VOCs than reported previously, have also not been explored.

In this paper, we investigated these aspects by preparing thick film titania photocatalyst (Degussa P-25 TiO_2) coated on glass supports viz. beads and Rasching rings. The TiO_2/glass supports were used in vapour phase degradation of high concentration of toluene,

* Corresponding author. Tel.: +91 712 2249885 402; fax: +91 712 2249900.
E-mail address: nn_rao@neeri.res.in (N.R. Neti).

1385-8947/$ – see front matter © 2010 Elsevier B.V. All rights reserved.
doi:10.1016/j.cej.2010.07.038

acetone and ethanol in a batch recirculation photoreactor. It is found that the TiO_2/glass supports comprising thick TiO_2 films demonstrate high photoactivity for degradation of the chosen substrates. A tentative mechanism for efficient photodegradation of VOCs is discussed based on the kinetic data, SEM/EDX data, effect of water vapour on photodegradation kinetics, and intermediate analysis.

2. Materials and methods

2.1. Materials

Analytical reagent grade hydrofluoric acid and nitric acid was used. Chromatography grade (Lichrosolv, 99.999%) toluene, ethanol, acetone and 2-propanol were purchased from E. Merck (India) Pvt. Ltd. Mumbai, India. De-ionized water was used (Millipore Elix 3 water purifier) for preparing reagents. The photocatalyst used was Degussa P-25-TiO_2 (80:20 anatase/rutile) with average primary particle size of 30 nm and a specific surface area about 50 $m^2\ g^{-1}$.

2.2. Glass supports and pretreatment

Soda glass beads (dia. = 3.0 mm) and Rasching rings (length = 6.0–8.0 mm, outer diameter 6 mm and inner diameter 4 mm) were obtained from a local vendor. The supports were thoroughly washed in a detergent solution and then etched in a solution containing 5% HF and 10% HNO_3 for 30 min. The etched supports were rinsed in water and dried in an oven at 100 °C for 12 h.

2.3. Preparation of TiO_2 coated supports

The photocatalyst (P-25 TiO_2, 5.0 g) was suspended in 100 mL of 20:80 water/2-propanol mixture. The suspension was magnetically stirred for 30 min to disperse the TiO_2 effectively. About, 670 g glass beads or 326 g Rasching rings (as required for loading into photoreactor), were taken separately into a glass tray and spread evenly and photocatalyst suspension was sprayed onto the supports while hot air was blown over them. The tray was gently shaken laterally to turn the supports around and ensure coating of photocatalyst on the surface of beads or Rasching rings. The coated supports were calcined at 150 °C for 1 h. The procedure was repeated five times to obtain thick and visibly uniform coating of TiO_2. All the suspension was consumed in the coating process. The TiO_2 coated glass beads and Rasching rings are referred as TiO_2/B and TiO_2/R, respectively.

The amount of TiO_2 coated on the supports was estimated from the difference in the weight of the supports before and after coating. This was also verified by using the digestion method described by Karches et al. [40] According to this method, 30 g of either TiO_2/B or TiO_2/R was digested in 100 mL concentrated H_2SO_4 containing 18 g $(NH_4)_2SO_4$ and the filtrate was analyzed for Ti concentration using an inductively coupled plasma-optical emission spectrometer (ICP-OES, Perkin Elmer, Model Optima 4100 DV).

2.4. Characterization of TiO_2 coated supports

Both TiO_2/B and TiO_2/R were characterized for surface morphology using Scanning Electron Microscopy (SEM) and TiO_2 layer was probed using Energy Dispersive X-ray Analysis (EDX). A Philips XL 30 CP Scanning Electron Microscope equipped with SE, BSE and Robinson detectors was used to observe changes in particle size and surface morphology. Neat powder samples were examined without conductive metal layer coating. Theoretical compositions of the samples were confirmed using EDX microanalysis (EDX detector/Genesis-2003, USA) attached to the SEM.

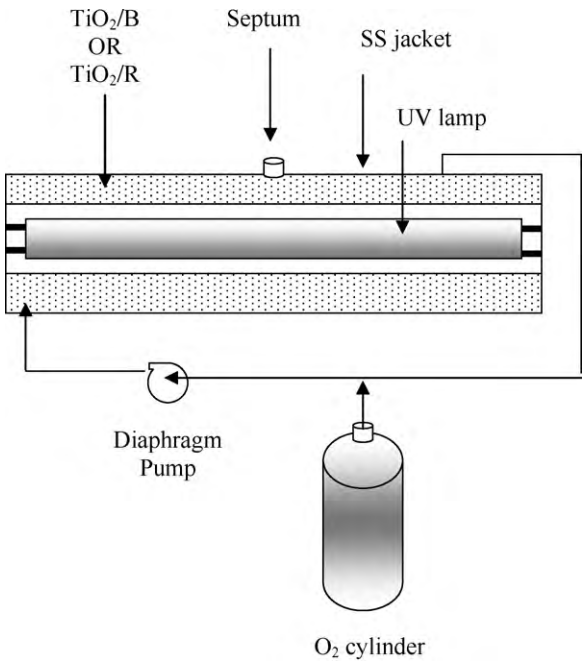

Fig. 1. Schematics of the batch recirculation photoreactor (BRPR).

2.5. Batch recirculation photoreactor (BRPR)

The TiO_2/glass supports were tested for their ability to photodegrade the VOCs by placing the supports in a gas-tight stainless steel (SS) vessel (length = 33 cm; dia. = 7.3 cm). A quartz tube of smaller dia. (5.4 cm) was placed inside the SS vessel. The gap between the outer SS vessel and quartz tube was 1.9 cm. The effective volume of the empty space between stainless steel vessel and quartz tube was 0.34 L. A germicidal high-pressure mercury lamp (AGUC 380 UV lamp G8T5, Phillips AG, 8W, peak emission wavelength at 254 nm, effective output intensity = 106 mW $cm^{-2}\ s^{-1}$) was placed inside the quartz tube for illuminating the coated supports. The light intensity measurements were made using a ILT 1700 Research Radiometer. One end of the reactor was sealed initially and the empty space was charged with TiO_2/glass supports. Then the other end of the reactor was also sealed using Teflon® lid. The outer surface of the photoreactor was wrapped with a thermo jacket (Flamingo) and the reactor temperature was maintained between 60 and 70 °C for complete volatilization of organic compounds. Gas inlet and outlet nozzles were fixed on the SS vessel as also a silicone septum for introducing and withdrawing samples periodically. A diaphragm pump with a fixed pumping rate of 1.0 L min^{-1} was used for circulating the gases. The schematic of the BRPR is given in Fig. 1.

2.6. Procedure for photocatalytic degradation

Initially, the batch recirculation photoreactor was charged with the photocatalyst coated support. About, 670 g of TiO_2/B or 326 g of TiO_2/R was required to fill the photoreactor. Then, the reactor was flushed for 15 min with oxygen to remove air-bound con-

Table 1
Analytical (GC) conditions for determination of toluene, acetone, and ethanol.

GC section	Temperature, °C		
	Toluene	Acetone	Ethanol
Oven	200	90	60
Injector	250	230	150
Detector	300	280	200

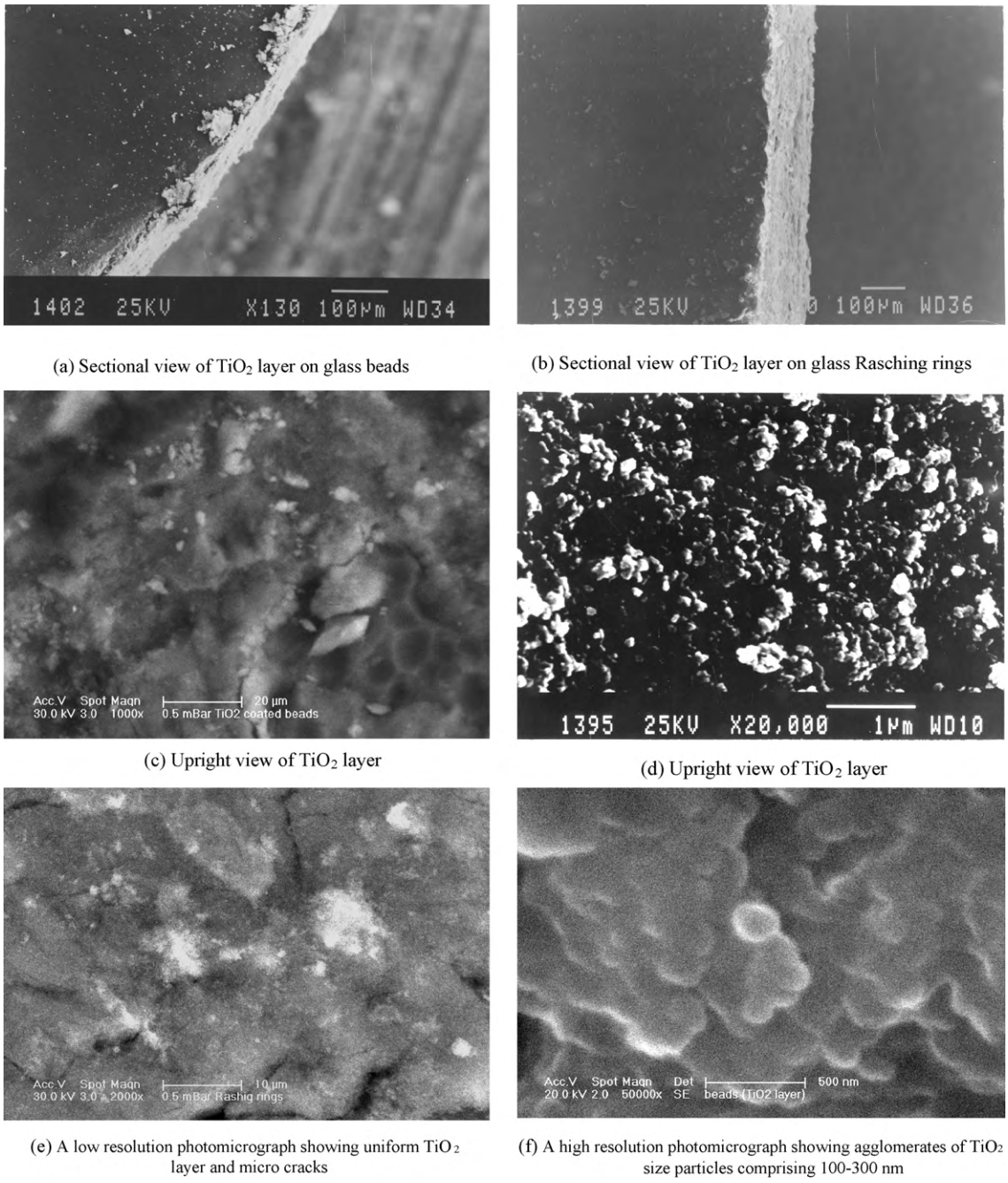

(a) Sectional view of TiO_2 layer on glass beads

(b) Sectional view of TiO_2 layer on glass Rasching rings

(c) Upright view of TiO_2 layer

(d) Upright view of TiO_2 layer

(e) A low resolution photomicrograph showing uniform TiO_2 layer and micro cracks

(f) A high resolution photomicrograph showing agglomerates of TiO_2 size particles comprising 100-300 nm

Fig. 2. (a and b) Cross-section of the TiO_2 layer on the glass beads and Rasching rings; (c–f) morphology of the TiO_2 layer on the glass beads and Rasching rings.

taminants from the reactor, and then filled with dry oxygen at atmospheric pressure. Then, the diaphragm pump was started and the reactor temperature was increased to 60 °C. Since the reactor contains solid supports the flow would be constricted and turbulent. A desired volume of VOC was then introduced into the system through a septum on the top of reactor and was volatilized. In each case, a small volume of VOC sample from the reactor was withdrawn at intervals to verify the contact time needed for attaining steady-state concentration of VOC. The UV lamp was started once the gas-solid adsorption equilibrium was established. Linearized Langmuir adsorption isotherms ($1/x$ vs. $1/C_e$) were constructed using the experimental mass of VOC adsorbed on TiO_2 (x) and equilibrium concentration of VOC (C_e) and adsorption constants (K, x_m) were deduced. The absorption constant K signifies affinity to adsorption and x_m denotes limiting adsorption concentration of VOC as per the Langmuir adsorption model.

The photo oxidation of VOC was determined by sampling the reactor gases periodically and analyzing the VOC concentration on a gas chromatograph (GC, Autosystem XL-Perkin Elmer). A 100-µL gas-tight pressure lock syringe (Hamilton make) was used for gas sampling. The concentration of VOCs was monitored using the GC equipped with glass lined injection port and flame ionization detector (FID). A stainless steel column of 2 m length and 0.313 cm internal diameter of 10% OV 101 silicone packed on chromosorb WHP of mesh 80/100 (Perkin Elmer) was used for separation. The carrier gas (N_2) flow was 5 mL min^{-1}. The VOC concentration data from duplicate runs were found reproducible within 2–5% error. The analytical GC conditions for the determination of toluene, acetone, and ethanol are given in Table 1.

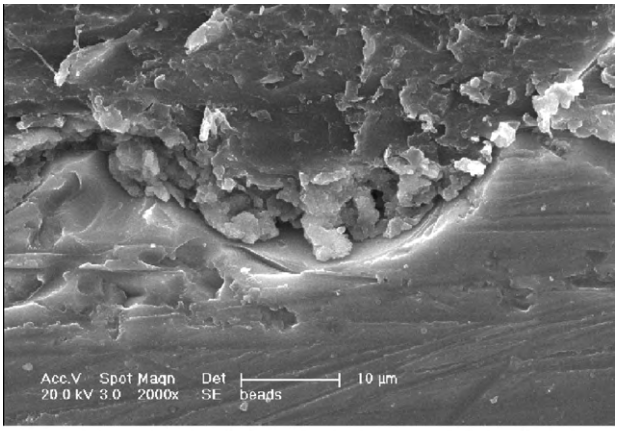

(a) Cross Sectional view of TiO_2 layer on glass beads

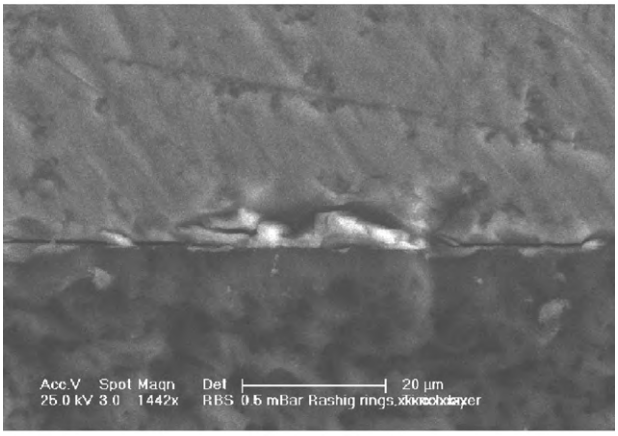

(b) Cross Sectional view of TiO_2 layer on Rasching Rings

Fig. 3. Interfaces between glass support-TiO_2 layer and resin-TiO_2 layer on the glass beads (a) and Rasching rings (b).

The photocatalytic activity of TiO_2/B and TiO_2/R was quantitatively evaluated by comparing the apparent rate constants (k_a). Following Langmuir–Hinshelwood mechanism, the k_a was deduced from the relation (Eq. (1)),

$$-\log(c_t/c_0) = k_a t, \quad (1)$$

where c_0 and c_t represent the initial and reaction concentrations of any of the chosen VOCs, respectively.

3. Results and discussions

3.1. Characterization of photocatalyst coated supports

The EDX data (not shown) showed the elemental composition (At %) of the soda glass supports as: Si (28.96), O (55.04), Na (9.84), Mg (2.09) and Ca (4.07). Thick films of TiO_2 were deposited over the beads as well as Rasching rings. The titania film on un-etched surface of the glass beads and Rasching rings was detached on wiping with a tissue paper. Repeatedly, scotch tape and fingernail scratch tests showed poor adherence of TiO_2 layer. On the other hand, the layer was quite adherent on etched surface of the chosen glass supports as observed by repeated scotch tape tests. However, some loosely bound TiO_2 powder from the surface over layer was removed during the initial handling which accounted for <2% TiO_2 loss.

The amount of TiO_2 per gram of the glass beads, as estimated from the weight difference was about 5.22×10^{-3} g. This amounts to 3.5 ± 0.1 g TiO_2 on 670 g glass beads required for filling the reactor. Similarly, the amount of TiO_2 per gram of Rasching rings was 9.20×10^{-3} g that works out as 3.0 g TiO_2 on 326 g Rasching rings required for charging the reactor. The corresponding values estimated by $(NH_4)_2SO_4$–H_2SO_4 method were found to be 3.25 and 2.89 g TiO_2 for glass beads and Rasching rings, respectively. Both the methods are comparable well within 10% error. The coating procedure resulted in glass supports having 60–70% of initial amount of TiO_2 used for preparing the suspension.

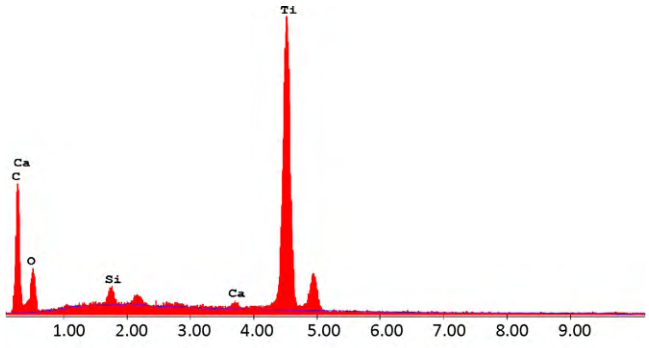

(a) EDX of TiO_2 layer on glass beads

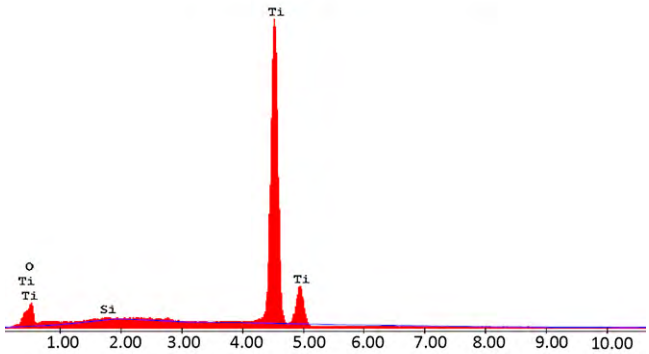

(b) EDX of TiO_2 layer on glass beads

Fig. 4. (a) EDX of the TiO_2 layer on the glass beads and (b) EDX of the TiO_2 layer on Rasching rings.

A cross-section of TiO_2 layer on the glass beads and Rasching rings is shown in Fig. 2(a and b). The thickness of the layer on the beads was found to be in the range of 45–50 μm whereas it was 100–110 μm thick on Rasching rings. The morphology of the TiO_2 layer is presented in Fig. 2(c–f). The photomicrograph in Fig. 2(c) illustrates an upright view of TiO_2 layer; in the background micron size pits on the glass formed due to etching can be seen. The surface of the etched glass beads is rough and the etch pits served as 'locks' for TiO_2 layer. Further, the upright view of the titania layer presented in photomicrograph Fig. 2(e), suggests thick layer with some microcracks. The layer also constituted a uniform dispersion of spherical shaped TiO_2 particles in the size range 100–300 nm (Fig. 2(d)). A few larger agglomerates of TiO_2 were also found. A high-resolution photomicrograph of a cross-section of titania layer revealed stacks of agglomerates; several nanoparticles appear to fuse together to form agglomerates (Fig. 2(f)).

In this study, the titania film coated on the glass beads and Rasching rings was calcined at 150 °C for 1 h. This was done deliberately to avoid migration of Na ions into titania layer induced by high temperatures. Such migration of Na and other native elements from soda lime glass could decrease photoactivity of titania films, which had been reported before [37,39,40]. Hence, SEM/EDX and mapping studies were performed to understand whether this hypothesis was correct. The interfaces between support-TiO_2 layer and resin-TiO_2 layers are depicted in Fig. 3(a and b). The EDX result is presented in

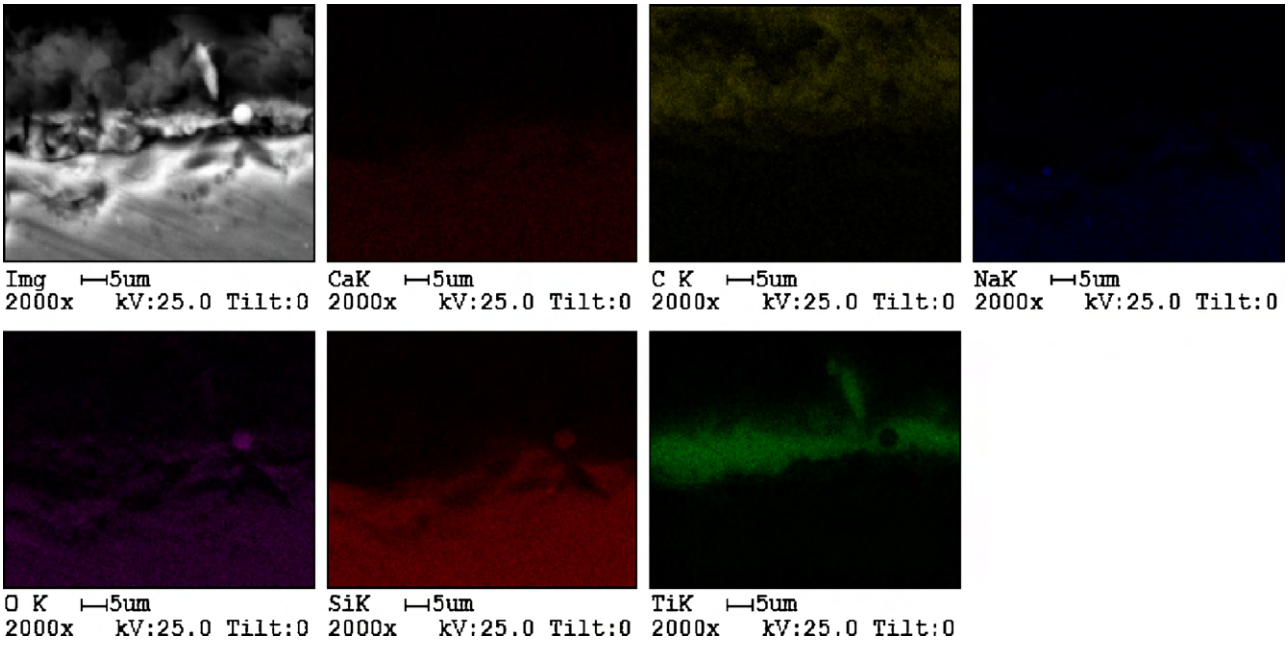

Fig. 5. EDX mapping of C, O, Si, Na, Ca, and Ti of TiO_2/B.

Fig. 4(a and b) for the TiO_2 layers on the glass beads and Rasching rings. The major phase was TiO_2. Some impurity of silicon was also identified, probably due to the exposed glass filings that may have lodged on to the TiO_2 layers. The mapping of C, O, Si, Na, Ca, and Ti of TiO_2/B is shown in Fig. 5. These elements were confined to their expected regions only. This also shows that Na did not diffuse into outer TiO_2 layer. Thus, migration of Na ions from soda lime glass supports into thick TiO_2 layer can be avoided by calcining the TiO_2/glass supports at a lower temperature.

3.2. Steady-state adsorption of toluene, acetone, and ethanol at TiO_2/glass supports

Initially, each of the above substrates was allowed to reach adsorption equilibrium with the catalyst separately in the BRPR before UV irradiation. This was assessed from the gas chromatograms that displayed comparable peak areas. All the three substrates showed adsorption at TiO_2/glass supports; however, the time required to attain equilibrium depended on the nature and the concentration of a VOC. Thus, 78–38% toluene in the concentration range of 63–383 g m^{-3}, 48.3–53% acetone in the concentration range of 116–1161 g m^{-3} and 74.9–47% ethanol in the concentration range of 116–1161 g m^{-3} were adsorbed on the photocatalyst supports.

Langmuir adsorption isotherms, regression coefficients (R^2), adsorption parameters (x_m, K) for toluene, acetone, and ethanol at TiO_2/R (amount of TiO_2 = 3.0 g) under the experimental conditions during attainment of adsorption equilibrium are given in Table 2. The adsorption of these compounds over TiO_2 fits to Langmuir adsorption model reasonably with the best fit line having R^2 value > 0.90. The relative affinities towards adsorption of these compounds on TiO_2 decreases in the order toluene ≫ ethanol > acetone, as is evident from the K values.

Table 2
Langmuir adsorption isotherms, regression coefficients (R^2), adsorption parameters (x_m, K) for toluene, acetone, and ethanol at TiO_2/R (amount of TiO_2 = 3.0 g) under the experimental conditions during attainment of adsorption equilibrium.

Substrate	Langmuir isotherm	R^2	x_m (μ moles)	K (μ moles)$^{-1}$
Toluene	$1/x = 0.3889 \times 1/C_e - 33.930$	0.93	0.0295	87.16
Acetone	$1/x = 1.061 \times 1/C_e - 1.638$	0.99	0.6106	1.54
Ethanol	$1/x = 0.2827 \times 1/C_e + 6.879$	0.97	0.1454	24.32

3.3. Photodegradation of toluene, acetone, and ethanol

Initially, blank reactivity tests were performed for all the three VOCs under the same experimental conditions used for photodegradation experiments but excluding either TiO_2/glass supports or UV light at a time. There was no decrease in the steady-state concentration of these substrates under both the conditions showing that both photocatalyst and UV light are necessary for the photodegradation of these substrates. The blank experiments also confirmed that VOCs did not leak from the photoreactor loop.

The variation of concentration of toluene, acetone, and ethanol with irradiation time for both TiO_2/B and TiO_2/R are depicted in Fig. 6. The concentration versus time profiles at different concentrations of each substrate are also illustrated. The concentration of all the substrates decreases exponentially with the increasing irradiation time, as expected for a typical first-order reaction. The values of k_a and regression coefficients (R^2) derived from $-\log[c_t/c_0]$ vs. time plots are given in Table 3(a–c). To compare the efficiency of degradation using TiO_2/B and TiO_2/R, the k_a at each concentration was normalized to the weight of TiO_2 catalyst in each case.

A maximum of 95.9 and 84% toluene was degraded during 90 min at the lowest (63.9 g m^{-3}) and the highest concentration (383.8 g m^{-3}). The k_a for the photodegradation of toluene was found to vary from 1.48×10^{-2} to 9.4×10^{-3} g m^{-3} min^{-1} (Table 3a). The k_a decreased with increasing toluene concentration up to 191.9 g m^{-3}, but it was practically invariant at higher concentrations. Based on the ratio of normalized k_a, which is close to unity at almost all the concentrations of toluene, both TiO_2/B and TiO_2/R may be said to show comparable photoactivity.

The photodegradation of acetone was nearly complete within 1 h with 83–93% efficiency in the concentration range of 116.2–580.9 g m^{-3}. The k_a for acetone photodegradation was found to vary from 5.57×10^{-2} to 1.29×10^{-2} g m^{-3} min^{-1} for TiO_2/B and 6.70×10^{-2} to 1.17×10^{-2} g m^{-3} min^{-1} for TiO_2/R (Table 3 b). The k_a decreased with the increase in acetone concentration following the first-order kinetics. The TiO_2/R showed somewhat higher pho-

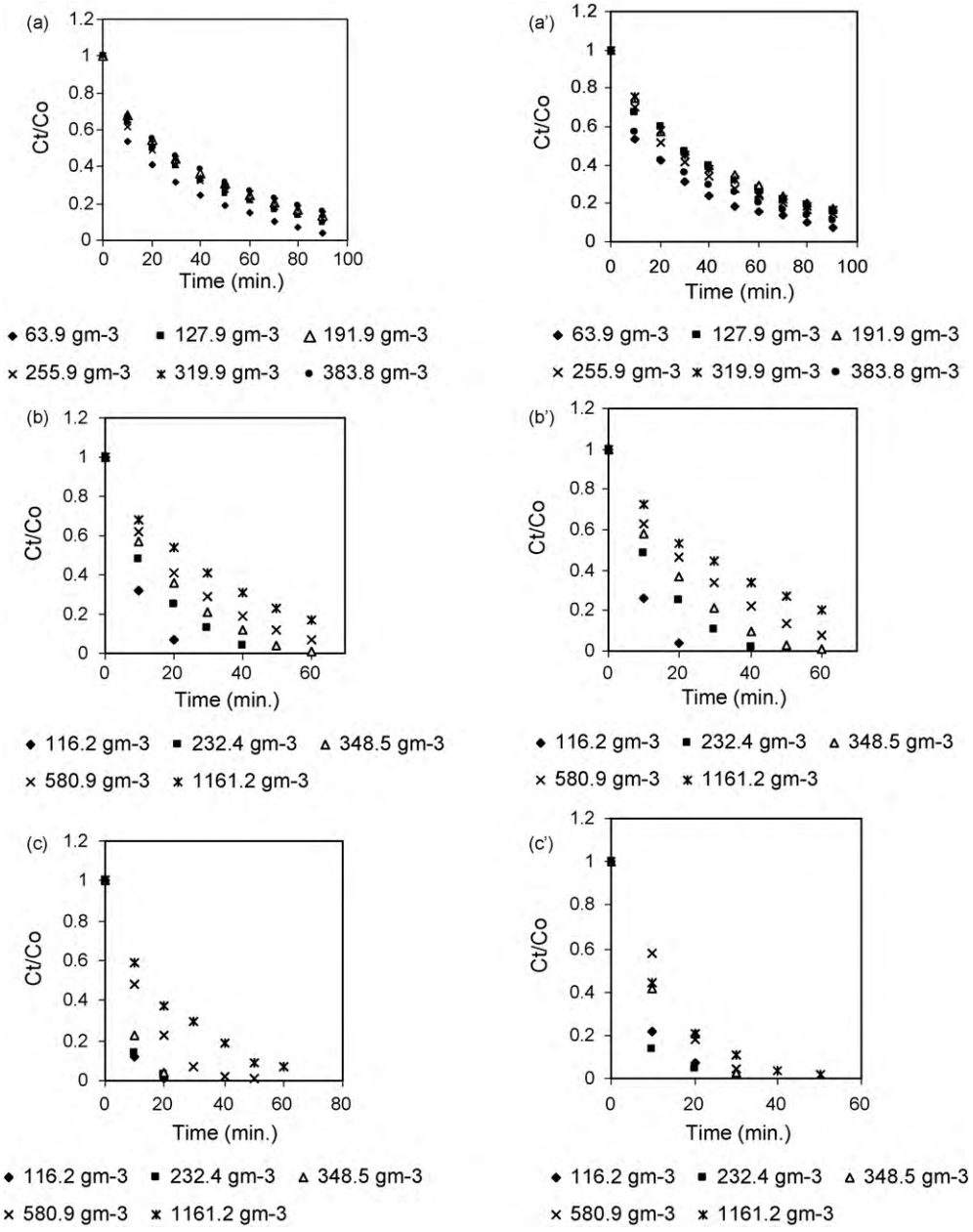

Fig. 6. Time course variation of concentrations (normalized) of toluene, acetone, and ethanol with irradiation time for TiO_2/B and TiO_2/R: (a) and (a') toluene on glass beads and Rasching rings; (b) and (b') acetone on glass beads and Rasching rings;(c) and (c') ethanol on glass beads and Rasching rings.

toactivity compared to that of TiO_2/B at least in the lower range of acetone concentration. However, k_a values for both the supports are comparable at higher concentrations of acetone.

Ethanol photodegraded with 99.3% efficiency within 10 min at 116.2 g m^{-3} using TiO_2/B. However, a 10-fold increase in ethanol concentration resulted in decrease of efficiency to 93.2%. On the other hand, the efficiency was 92.8% with TiO_2/R. The photodegradation efficiency was higher than 96% in ethanol concentration range of 116–580.9 g m^{-3}. The k_a for ethanol photodegradation using TiO_2/B was found to vary from 2.14×10^{-1} to 1.96×10^{-2} g m^{-3} min^{-1} and 7.25×10^{-2} to 3.51×10^{-2} g m^{-3} min^{-1} using TiO_2/R. The TiO_2/B showed three times higher photoactivity compared to that of TiO_2/R at the lowest ethanol concentration. However, the TiO_2/R showed higher photoactivity at the higher concentrations of ethanol.

Based on the k_a data in Table 3(a–c), the observed order of photodegradation is inferred as ethanol > acetone > toluene. The k_a for the photodegradation of ethanol at TiO_2/B is 14- and 3.8-folds higher than that of toluene and acetone, respectively at the lowest concentration of the substrates explored in this study. Under similar conditions, the use of TiO_2/R resulted in 4.5 times higher k value for ethanol degradation in comparison to toluene. The photodegradation rates for acetone and ethanol at both TiO_2/B and TiO_2/R are comparable. This shows that the aromatic compounds such as toluene are more difficult to photodegrade when compared to the aliphatic compounds having fewer carbon atoms. The rate constants normalized to the weight of TiO_2 on the total weight of either TiO_2/B or TiO_2/R in the reactor, are comparable, barring a few cases, e.g. $k_{a(\text{ethanol, } 116.2\,\text{g m}^{-3})}$ is three times higher on TiO_2/B when compared to that of TiO_2/R.

The above results indicate somewhat higher photodegradation efficiency using TiO_2/R. This may be attributed to difference in packing patterns and associated radiation characteristics. As mentioned in the experimental section the supports were packed into

Table 3
Photocatalytic degradation of toluene, acetone, and ethanol.

(a) Photocatalyst	[Toluene] ($g\,m^{-3}$)	63.9	127.9	191.9	255.9	319.9	383.8
TiO_2/B	k ($\times10^{-2}$ min^{-1})	1.48	1.14	1.01	1.08	1.00	0.94
	(R^2)	0(.98)	0(.98)	0(.98)	0(.96)	0(.96)	0(.96)
	k_n(B), ($\times10^{-2}$ min^{-1}/g)[a]	0.422	0.325	0.288	0.308	0.285	0.268
TiO_2/R	k ($\times10^{-2}$ min^{-1})	1.31	0.93	0.89	1.01	0.95	1.14
	(R^2)	0(.93)	0(.97)	0(.97)	0(.95)	0(.97)	0(.92)
	k_n(R), ($\times10^{-2}$ min^{-1}/g)[a]	0.436	0.310	0.296	0.336	0.316	0.380
k_n(B)/k_n(R)		0.96	1.05	0.97	0.91	0.90	0.70

(b) Photocatalyst	[Acetone] ($g\,m^{-3}$)	116.2	232.4	348.5	580.9	1161.2
TiO_2/B	k ($\times10^{-2}$ min^{-1})	5.57	2.99	2.49	1.87	1.29
	(R^2)	0(.99)	0(.99)	0(.98)	0(.99)	0(.99)
	k_n(B),($\times10^{-2}$ min^{-1}/g)[a]	1.59	0.854	0.711	0.534	0.368
TiO_2/R	k ($\times10^{-2}$ min^{-1})	6.70	3.77	3.11	1.75	1.17
	(R^2)	0(.99)	0(.94)	0(.90)	0(.98)	0(.99)
	k_n(R), ($\times10^{-2}$ min^{-1}/g)[a]	2.23	1.25	1.03	0.58	0.39
k_n(B)/k_n(R)		0.71	0.68	0.69	0.92	0.94

(c) Photocatalyst	[Ethanol] ($g\,m^{-3}$)	116.2	232.4	348.5	580.9	1161.2
TiO_2/B	k ($\times10^{-2}$ min^{-1})	21.41	8.02	6.96	3.87	1.96
	(R^2)	(1)	0(.99)	0(.99)	0(.99)	0(.99)
	k_n(B), ($\times10^{-2}$ min^{-1}/g)[a]	6.11	2.29	1.98	1.10	0.56
TiO_2/R	k ($\times10^{-2}$ min^{-1})	5.91	7.25	4.60	4.18	3.51
	(R^2)	0(.99)	0(.97)	0(.93)	0(.95)	0(.99)
	k_n(R), ($\times10^{-2}$ min^{-1}/g)[a]	1.97	2.41	1.53	1.39	1.17
k_n(B)/k_n(R)		3.10	0.95	1.29	0.79	0.47

[a] Normalized rate constant, [k_n(B) or k_n(R)] = k/(weight of TiO_2 on glass beads (3.5 g) or (weight of TiO_2 on Rasching rings (3.0 g).

the reactor having gap of 1.9 cm between outer SS jacket and inner quartz tube. The photoreactor volume was 0.34 L. In the absence of packed supports, the reaction zone was fully illuminated with UV light. However, when the reaction zone was packed with TiO_2/B or TiO_2/R, we may expect some gradient in radiation characteristics; the illumination intensity may diminish across the gap, it being more intense at inner quartz tube and less intense at outer SS jacket. In separate experiments that involved use of photoreactor having borosilicate glass outer jacket, we determined drop in intensity of light across the depth (gap) of the packed reactor. The light intensity at the outer edge of the borosilicate jacket was 74 and 91 $mW\,cm^{-2}\,s^{-1}$ using TiO_2/B and TiO_2/R, respectively as against its actual output of 106 $mW\,cm^{-2}\,s^{-1}$ in the absence of packed bed. This can be attributed to the difference in packing patterns of glass beads and Rasching rings, in the photocatalytic reactor as depicted in Fig. 7. In the case of glass beads (Fig. 7(a)), the solid spheres adopt a denser and orderly packing leaving lesser void space. Therefore, the UV light in this case may be partially blocked by the dense packing of solid glass beads as a result glass beads located away from the middle of the reactor will receive less radiation. In contrast, the packing of Rasching rings

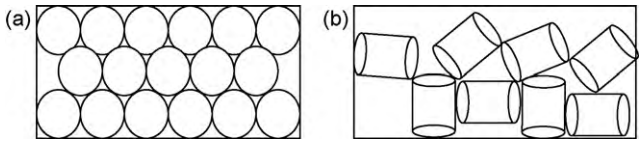

Fig. 7. Possible packing patterns of glass supports in the photoreactor (a) TiO_2/B and (b) TiO_2/R.

can be expected to be random with low density because they are hollow and cylindrical (Fig. 7(b)). This may also provide for more exposed area for the UV light in the packed zone. Accordingly, drop in UV intensity in the case of TiO_2/R was less. Thus, TiO_2/R appear to show better photodegradation efficiency in comparison with TiO_2/B because their packing favours exposure of more surface and better illumination in the reactor. Moreover, their low density packing implies lesser weight of the photoreactor.

Table 4
Degradation time for substrates and intermediates formed during photodegradation.

Concentration ($g\,m^{-3}$)		Degradation time (min)					
		Toluene		Ethanol		Acetone	
Toluene	Ethanol/acetone	Toluene	BA[a]	Ethanol	AA[b]	Acetone	–
63.9	116.2	120	90	20	30	30	No intermediate
127.9	232.4	130	140	30	50	50	
191.9	348.5	170	170	30	50	70	
255.9	580.9	190	200	60	90	90	
319.9	1161.2	250	210	180	270	130	
383.8	–	250	220				

[a] Benzaldehyde (appears after 10 min irradiation).
[b] Acetaldehyde (appears after 10 min irradiation).

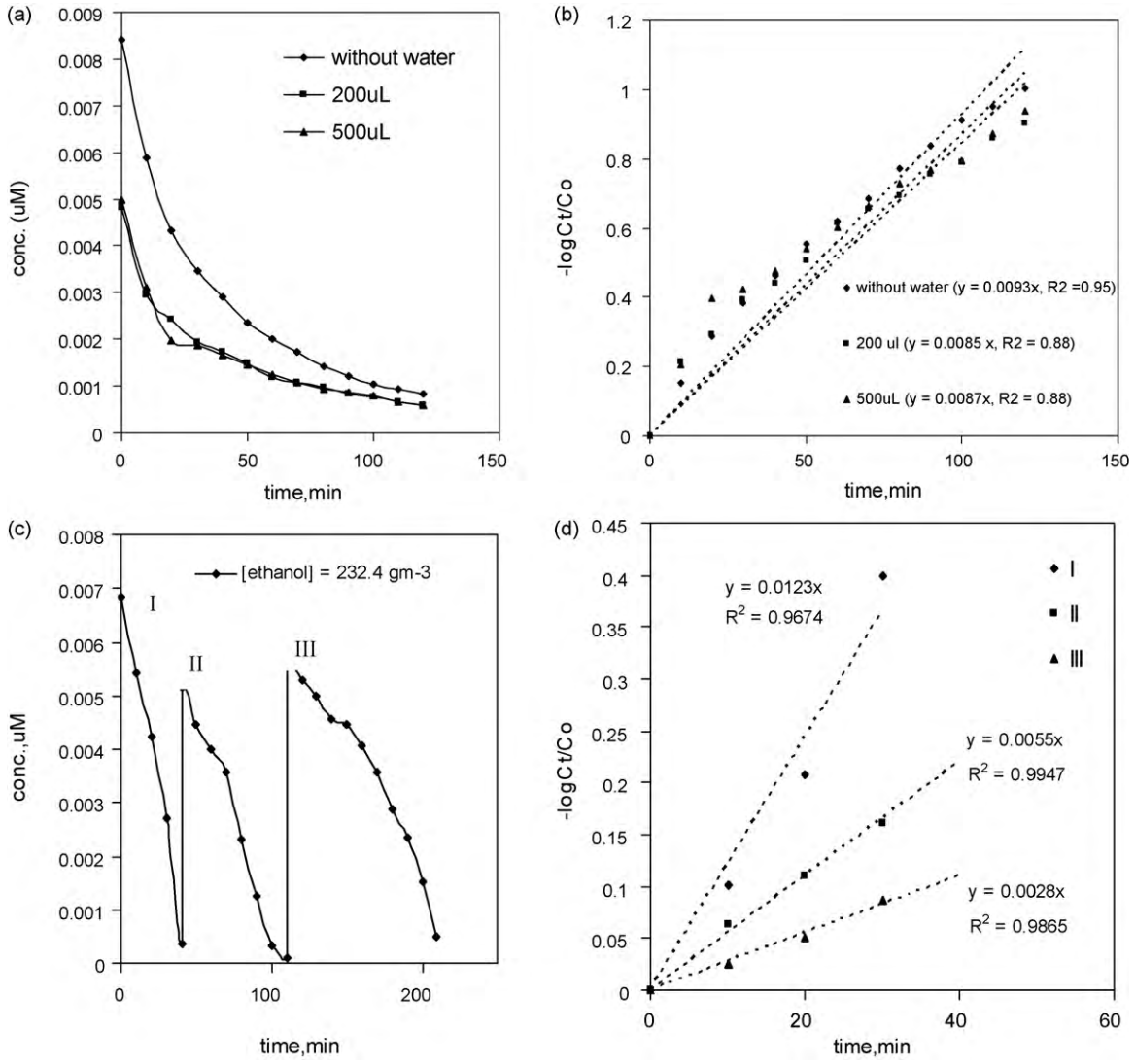

Fig. 8. Influence of water vapour on the photodegradation of (a and b) toluene and (c and d) ethanol.

3.4. vapour phase intermediates

Benzaldehyde and acetaldehyde were detected in the vapour phase during photodegradation of toluene and ethanol, respectively. Acetone photodegraded entirely to carbon dioxide and water. The illumination period after which these intermediates were detected and the time required for their degradation is presented in Table 4. The concentrations and the degradation time of original substrates are also presented for comparison. Benzaldehyde was detected after 10 min illumination. This was oxidized completely along with toluene. On the other hand, the photodegradation of acetaldehyde was slower than that of ethanol, it required more than 4 h for complete photodegradation under the experimental conditions in the present study.

3.5. Influence of water vapour on the photodegradation kinetics

Humidity in the photoreactor often influences the photodegradation processes. It can contribute to surface rehydration of photocatalyst that may lead to increase in concentration of OH radicals and hence increase in reaction rate. Competitive adsorption between water vapour and the organic compounds is also common at higher water vapour content. Therefore, the effect of water vapour on the photodegradation of toluene and ethanol was studied.

Fig. 8 depicts the effect of water vapour on photodegradation of toluene (a and b) and ethanol (c and d) at their representative concentrations of 256 g m^{-3} and 232.4 g m^{-3}, respectively. The concentration vs. time profiles of toluene with and without added water shown in Fig. 8(a) are typical of first-order reaction kinetics. The steady-state concentration of toluene in the gas phase was somewhat less in the presence of added water vapour. The corresponding rate constants (Fig. 8(b)) for photodegradation of toluene at 200 and 500 mg m^{-3} of water were estimated as $k_{200} = 8.5 \times 10^{-3}$ min^{-1} and $k_{500} = 8.7 \times 10^{-3}$ min^{-1}, while the original rate constant without added water vapour was $k_0 = 9.3 \times 10^{-3}$ min^{-1}. The reaction is slightly inhibited in the presence of water vapour. Interestingly, benzaldehyde was not detected in the presence of added water vapour, which can be attributed to preferred formation of less reactive benzoic acid intermediate. The FTIR spectra of the recovered TiO_2 showed peaks at 1716, 1400–1500 cm^{-1} that can be attributed to benzoic acid. The observed inhibition of toluene photodegradation in the presence of water vapour may be due to adsorption of benzoic acid molecules that cause deactivation of the photocatalyst. Several authors have also reported benzoic acid adsorption on TiO_2 surface [20,21].

It was observed that water vapour accumulated in the reactor loop during ethanol photodegradation. Therefore, the effect of water was examined by injecting fresh doses of ethanol into the photoreactor. It was assumed that water vapour formed in each batch is additive. Fig. 8(c and d) present the photodegradation of fresh doses (I, II, and III batches) of ethanol. The corresponding first-order plots (Fig. 6(d)) show that $k_I = 1.23 \times 10^{-2}\,g\,m^{-3}\,min^{-1}$, $k_{II} = 5.50 \times 10^{-3}\,g\,m^{-3}\,min^{-1}$, $k_{III} = 2.80 \times 10^{-3}\,g\,m^{-3}\,min^{-1}$. This data suggests significant inhibition of photodegradation of ethanol in the presence of water vapour, which can be attributed to competitive adsorption described earlier. The rate of photodegradation of several VOCs including toluene and ethanol [20,28,29] has been reported to be dependent on their functional groups and chemical structures and on the ratio between concentrations of VOCs and water vapour.

3.6. Mechanistic aspects

In this study, it is observed that toluene, acetone, and ethanol adsorb on TiO_2/glass supports and undergo photo oxidation following the first-order kinetics. This is frequently true for the photocatalytic degradation of many organic compounds [41]. This may involve direct oxidation by photo-generated holes or indirect oxidation promoted by formation of hydroxyl radicals on the surface of illuminated titania [1–4]. Under these circumstances, it is well-known that photo oxidation of organic substrates on illuminated TiO_2 proceeds through photo generation of OH radicals, adsorption of organic substrates, and reaction between OH radicals and adsorbed organic compounds.

Davit et al. [41] reported that toluene adsorption on P-25-TiO_2 surface was accompanied with the decrease in IR absorption due to free OH groups at 3700–3600 cm^{-1}, and that the free OH groups act as Lewis acid adsorption sites involving weak interaction between OH groups and π-electrons of toluene molecules. A study [23] has reported dimerization of acetone on the surface of TiO_2, especially at higher surface coverage. The dimerization product, mesityl oxide, is reported to undergo slower photo oxidation as compared to acetone. Adsorbed ethanol on TiO_2 has been reported to exist as hydrogen bonded ethanol species and surface-bound Ti-ethoxide [28]. The adsorption and types of intermediates formed are also influenced by humid air or water which readily hydrates the surface of titania.

It is pertinent to compare the reported rate constants for vapour phase photodegradation of toluene, acetone, and ethanol, with the k_a values found in the present study. Wherever possible, the reported k values were converted into $g\,m^{-3}\,min^{-1}$ and are given in parenthesis for comparison. Kim and Hong [24] and Kim et al. [11] have reported photodegradation of acetone and toluene over thin films (65 nm) of TiO_2 on Pyrex glass tubes in batch recirculation reactor. The k were $2.2 \times 10^{-3}\,mol\,m^{-3}\,min^{-1}$ ($0.128\,g\,m^{-3}\,min^{-1}$) and $4.5 \times 10^{-4}\,mol\,m^{-3}\,min^{-1}$ ($4.14\,g\,m^{-3}\,min^{-1}$) for acetone ($C_0 = 1.04\,g\,m^{-3}$) and toluene ($C_0 = 0.69\,g\,m^{-3}$), respectively. These authors [11,24] reported that the rate of degradation of acetone was retarded due to competitive adsorption of water on titania, while it increased the rate of photodegradation of toluene due to desorption of benzoic acid intermediate in the presence of water. Maria et al. [19] examined the influence of the titania particle size (6, 11, 16, and 20 nm) applied as a thin film over Pyrex tubes on the photodegradation of toluene ($C_0 = 0.06$–$0.15\,mmol\,dm^{-3}$ i.e. 5.52–13.8 $g\,m^{-3}$). The rates varied from 0.5 to $1.0 \times 10^{-9}\,mol\,s^{-1}\,m^{-2}$; with smaller particle sizes leading to higher rates of photodegradation of toluene. Addition of water increased the percent conversion of toluene by 2–3 times. Arana et al. [28] reported photodegradation of ethanol using packed bed P-25 TiO_2 photocatalyst. Acetaldehyde and ethylene glycol were identified and quantified, the fluxes were found to vary from 1.0×10^{-3} to $4.2 \times 10^{-3}\,mmol\,g^{-1}\,cat\,min^{-1}$. These authors discussed a two-site adsorption model according to which an ethanol molecule is chemisorbed through OH site on the surface. The chemisorbed ethanol molecule exists as an adsorbed ethoxide group due to release of a water molecule. Since water accumulation was observed during photodegradation of ethanol, a similar adsorption mechanism may be expected in the present case also. Piera et al. [29] reported photodegradation of gas phase ethanol ($C_0 = 48\,mg\,m^{-3}$) on P-25 TiO_2 spread over fritted glass plate. The k was equal to $0.086\,mg\,m^{-3}\,min^{-1}$. The main degradation product, acetaldehyde, has been reported to degrade 4–5 times slow. This is in accordance with the observations pertinent to ethanol photodegradation in the present study.

In the present study, the k_a (using TiO_2/B) for the photodegradation of toluene was found to vary from 1.48×10^{-2} to $9.4 \times 10^{-3}\,g\,m^{-3}\,min^{-1}$ (Table 3a); for acetone photodegradation from 5.57×10^{-2} to $1.29 \times 10^{-2}\,g\,m^{-3}\,min^{-1}$ (Table 3b), and for ethanol photodegradation from 2.14×10^{-1} to $1.96 \times 10^{-2}\,g\,m^{-3}\,min^{-1}$ (Table 3c). The k values are significantly higher than the previously reported data, especially when 10–100 times higher initial concentrations of the VOCs are considered. This can be attributed to thick films of TiO_2 obtained on the glass beads or Rasching rings that provided more amount of active sites for adsorption of the substrates. We found that the chosen VOCs were adsorbed on the photocatalyst supports significantly, which also reflects on the magnitude of active sites in the thick TiO_2 layers.

The migration of Na ions from soda lime glass supports into thick TiO_2 layer if any may have confined to glass/TiO_2 interface only, although much lower calcination temperature (150 °C) used in this study would have limited such migration, when compared with much higher calcination temperature adopted by some authors [37,43,44]. The EDX and mapping data suggest the absence of migration of Na ions into thick titania layer especially into the outer surface of TiO_2 layers. Many authors [37,42,43] attributed lower photoactivity of TiO_2/soda glass to Na migration. For example, Guillard et al. [37] found very similar photocatalytic activities for TiO_2 coated silicon wafer and Pyrex, whereas a 6-fold smaller activity was observed on soda lime glass. This difference was ascribed to the presence of cation (Na^+, Mg^{2+}, Ca^{2+}) in soda lime glass. In this case the TiO_2 coating thickness was between 0.15 and 1.5 μm, two orders of magnitude smaller than in the present study.

In the light of the above, it appears that titania thick films as in the present study showed higher photodegradation efficiencies through favoured adsorption and photodegradation of VOCs. This is also probably assisted by the higher temperature maintained in the photoreactor. The thickness of TiO_2 coating on glass beads and Rasching rings was about 50 and 100 μm, respectively. It is expected that UV radiation penetrates only a fraction of micrometers into the thick films. Generally, this depth is about 0.1 μm; however, Choi et al. [44] estimated the light penetration depth to be 0.78 μm during their studies to illustrate the effect of TiO_2 coating mass or thickness on the photodegradation of polychlorinated dibenzo-*p*-dioxins. Therefore, in the case of TiO_2/B or TiO_2/R, we may imagine existence of hypothetical regions of illuminated TiO_2 layer, a layer of TiO_2 not receiving radiation but can act as adsorbent for VOCs due to porous nature of the coated films. The functioning of thick films of TiO_2 on glass beads and Rasching rings may be understood with the illustration in Fig. 9. Accordingly, each TiO_2/glass beads/or Rasching rings may posses three different reaction zones under illumination namely (i) 'photoactive zone', which is the outer surface of TiO_2 coating receiving UV illumination presumably < 1.0 μm thick (ii) adsorption zone, which is bulk of TiO_2 underneath the photoactive zone and, (iii) glass/TiO_2 interface at which Na migration can be expected at higher calcinations temperatures. However, under UV illumination which penetrates a fraction of μm into TiO_2 thick layer wherein primary charge carriers (e^-_{CB} and h^+_{VB}) are generated is the photoactive zone. The primary charge

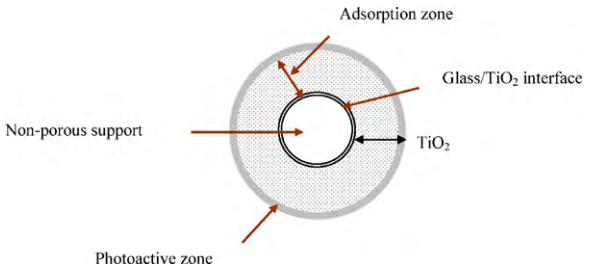

Fig. 9. Illustration of three different reaction zones on thick film TiO_2/glass supports under illumination depicting photoactive zone, adsorption zone, glass/TiO_2 interface.

carriers have very short lifetime of the order of nanoseconds; unless they are used up soon after their formation. Only a part of the photogenerated e^-_{CB} and h^+_{VB} migrate on to the surface whereby adsorbed oxygen and hydroxyl/water groups trap them. In suitable cases, they may directly react with adsorbed VOC molecules also. These reaction steps may be simplified as in the following:

$$(TiO_2)_{surface} + h\nu \rightarrow TiO_2\,(e^-_{cb} - h^+_{vb})$$

$$h^+_{VB} + (OH)_{ads}/(H_2O)_{ads} \rightarrow {}^\bullet OH$$

$$e^-_{CB} + (O_2) \rightarrow O_2{}^{-\bullet} \rightarrow H_2O_2 \rightarrow {}^\bullet OH$$

$$h^+ + VOC \rightarrow \text{Oxidation products}$$

$$VOC + {}^\bullet OH \rightarrow \text{Oxidation products}$$

The VOCs adsorbed in the adsorption zone underlying the photoactive zone migrate into photoactive zone and undergo photodegradation. This migration and photodegradation processes may have been aided by the higher temperature of the reactor (60–70 °C). The photoactive surface is continuously renewed and fresh VOC molecules undergo adsorption and photodegradation. This way, the adsorption, migration and photoreactions take place in tandem and contribute to higher photocatalytic VOC removal efficiencies.

4. Conclusion

Experiments were carried out on vapour phase photodegradation of high concentration of toluene, acetone and ethanol in a batch recirculation photoreactor comprising thick film (50–100 μm) titania photocatalyst (Degussa P-25 TiO_2) coated on glass supports viz. beads and Rasching rings. The following conclusions can be made from the present investigations:

- The VOCs undergo efficient photodegradation following the first-order kinetics. The rate constants (k_a) for photodegradation of toluene vary from 1.48×10^{-2} to 9.4×10^{-3} g m^{-3} min^{-1}; 5.57×10^{-2} to 1.29×10^{-2} g m^{-3} min^{-1} for acetone; and 2.14×10^{-1} to 1.96×10^{-2} g m^{-3} min^{-1} for ethanol using TiO_2/B. The k_a values using the TiO_2/R are of the same order. The k_a values for photodegradation of these substrates are significantly higher than those reported before in similar investigations.
- During the photodegradation of toluene and ethanol, benzaldehyde and acetaldehyde were detected in the vapour phase, respectively; however, they too undergo photodegradation simultaneously. Acetone photo degrades completely to carbon dioxide and water under the experimental conditions maintained in the present study.
- The functioning of the thick films of TiO_2 on glass beads and Rasching rings can be explained in terms of the existence of three different reaction zones under illumination namely (i) 'photoactive zone', which is the outer surface layer of TiO_2 coating receiving UV illumination presumably <1.0 μm thick (ii) adsorption zone, which is bulk of TiO_2 underneath the photoactive zone and, (iii) glass/TiO_2 interface at which Na migration can be expected at higher calcinations temperatures.
- The higher photodegradation efficiencies and excellent tolerance of the photoreactor to high concentrations of the VOCs can be attributed to more amounts of active sites provided by the thick TiO_2 films and favoured adsorption of and degradation VOCs assisted by the higher temperature maintained in the photoreactor.
- The TiO_2/R appear to show better photodegradation efficiency in comparison with TiO_2/B because their packing favours exposure of more surface and better illumination in the reactor. Moreover, their low density packing implies lesser weight of the photoreactor.

Acknowledgements

The authors (NNR) acknowledges the NREF grant from the Ministry of New and Renewable Energy (MNRE) New Delhi, India and partial funding under SIP-16 (3.2), CSIR, India. The authors also thank Director, NEERI, and Dr. Tapas Nandy, Scientist & Head, WWT for encouragement.

References

[1] D. Bahnemann, Photocatalytic water treatment: solar energy applications, Sol. Energy 77 (2004) 445.
[2] A. Fujishima, T.N. Rao, D.A. Tryk, Titanium dioxide photocatalysis, J. Photochem. Photobiol. C 1 (2000) 1.
[3] M.R. Hoffman, S.T. Martin, W. Choi, D.W. Bahnemann, Environmental applications of semiconductor photocatalysis, Chem. Rev. 95 (1995) 69.
[4] O. Legrini, E. Oliveros, A.M. Braun, Photochemical processes for water treatment, Chem. Rev. 93 (1993) 671.
[5] S. Malato, J. Blanco, A. Vidal, C. Richter, Photocatalysis with solar energy at a pilot-plant scale: an overview, Appl. Catal. B: Environ. 37 (2002) 1.
[6] N.N. Rao, S. Dube, Photocatalytic degradation of Reactive Orange 84 (RO84) in dye house effluent using single-pass reactor, Stud. Surf. Sci. Catal. 113 (1998) 1045.
[7] N.N. Rao, A. Dubey, R. Jain, P. Khare, S. Mohanty, S.N. Kaul, Photocatalytic degradation of 2-chlorophenol: a study of kinetics, intermediates and biodegradability, J. Hazard. Mater. 101 (2003) 301.
[8] S. Wang, H.M. Ang, M.O. Tade, Volatile organic compounds in indoor environment and photocatalytic oxidation: state of the art, Environ. Int. 33 (2007) 694.
[9] W.A. Jacoby, D.M. Blake, J.A. Fennell, J.E. Boulter, L.M. Vargo, M.C. George, S.K. Dolberg, Heterogeneous photocatalysis for control of volatile organic compounds in indoor air, Air Waste Manage. Assoc. 46 (1996) 891.
[10] G.-M. Zuo, Z.-X. Cheng, H. Chen, G.-W. Li, T. Miao, Study on photocatalytic degradation of several volatile organic compounds, J. Hazard. Mater. 128 (2006) 158.
[11] S.B. Kim, H.T. Hwang, S.C. Hong, Photocatalytic degradation of volatile organic compounds at the gas–solid interface of a TiO_2 photocatalyst, Chemosphere 48 (2002) 437.
[12] R.M. Alberici, W.F. Jardim, Photocatalytic destruction of VOCs in the gas-phase using titanium dioxide, Appl. Catal. B: Environ. 14 (1997) 55.
[13] M. Keshmiri, T. Troczynski, M. Mohseni, Oxidation of gas phase trichloroethylene and toluene using composite sol–gel TiO_2 photocatalytic coatings, J. Hazard. Mater. 128 (2006) 130.
[14] J. Jeong, K. Sekiguchi, K. Sakamoto, Photochemical and photocatalytic degradation of gaseous toluene using short wavelength UV irradiation with TiO_2 catalyst: comparison of three UV sources, Chemosphere 57 (2004) 663.
[15] T. Sano, N. Negishi, K. Takeuchi, S. Matsuzawa, Degradation of toluene and acetaldehyde with Pt-loaded TiO_2 catalyst and parabolic trough concentrator, Sol. Energy 77 (2004) 543.
[16] C. Belver, M.J. Lopez-Munoz, J.M. Coronado, J. Soria, Palladium enhanced resistance to deactivation of titanium dioxide during the photocatalytic oxidation of toluene vapours, Appl. Catal. B: Environ. 46 (2003) 497.
[17] Z. Pengyi, L. Fuyan, Y. Gang, Z. Chen Qing, Wanpeng, A comparative study on decomposition of gaseous toluene by O3/UV, TiO_2/UV and O3/TiO_2/UV, J. Photochem. Photobiol. A: Chem. 156 (2003) 189.
[18] A. Bouzaza, A. Laplanche, Photocatalytic degradation of toluene in the gas phase: comparative study of some TiO_2 supports, J. Photochem. Photobiol. A: Chem. 150 (2002) 207.

[19] A.J. Maria, K.L. Yeung, J. Soria, J.M. Coronado, C. Belver, C.Y. Lee, V. Augugliaro, Gas-phase photo-oxidation of toluene using nanometer-size TiO_2 catalysts, Appl. Catal. B: Environ. 29 (2001) 327.
[20] G. Martra, S. Coluccia, L. Marchese, V. Augugliaro, V. Loddo, L. Palmisano, M. Schiavello, The role of H_2O in the photocatalytic oxidation of toluene in vapour phase on anatase TiO_2 catalyst: a FTIR study, Catal. Today 53 (1999) 695.
[21] R. Mendez-Roman, N. Cardona-Martinez, Relationship between the formation of surface species and catalyst deactivation during gas-phase photocatalytic oxidation of toluene, Catal. Today 40 (1998) 353.
[22] M. El-Maazawi, A.N. Finken, A.B. Nair, V.H. Grassian, J. Catal. 191 (2000) 138.
[23] W. Choi, J.Y. Ko, H. Park, J.S. Chung, Investigation on TiO_2-coated optical fibers for gas-phase photocatalytic oxidation of acetone, Appl. Catal. B: Environ. 31 (2001) 209.
[24] S.B. Kim, S.C. Hong, Kinetic study of photocatalytic degradation of volatile organic compounds in air using thin film TiO_2 photocatalyst, Appl. Catal. B: Environ. 35 (2002) 305.
[25] J. Peral, D.F. Ollis, Photocatalytic oxidation of gas-phase organics for air purification, J. Catal. 136 (1992) 554.
[26] M.L. Sauer, D.F. Ollis, Acetone oxidation in a monolith reactor, J. Catal. 149 (1994) 81.
[27] T.H. Lim, S.D. Kim, Trichloroethylene degradation by photocatalysis in annular flow and annulus fluidized bed photoreactors, Chemosphere 54 (2004) 305.
[28] J. Arana, J.M. Dona-Rodriguez, O. Gonzalez-Diaz, E. Tello Rendon, J.A. Herrera Melian, G. Colon, J.A. Navio, J. Perez Pena, Gas-phase ethanol photocatalytic degradation study with TiO_2 doped with Fe, Pd and Cu, J. Mol. Catal. A: Chem. 215 (2004) 153.
[29] E. Piera, J.A. Ayllon, X. Domenech, Jose Peral, TiO_2 deactivation during gas-phase photocatalytic oxidation of ethanol, Catal. Today 76 (2002) 259.
[30] J.M. Coronado, S. Kataoka, I. Tejedor-Tejedor, M.A. Anderson, J. Catal. 219 (2003) 219.
[31] Darrin S. Muggli, Sheldon A. Larson, John L. Falconer, Photocatalytic oxidation of ethanol: isotopic labeling and transient reaction, J. Phys. Chem. 100 (1996) 15886.
[32] Darrin S. Muggli, Justin T. McCue, John L. Falconer, Mechanism of the photocatalytic oxidation of ethanol on TiO_2, J. Catal. 173 (1998) 470.
[33] O. Yoshihisa, D.A. Tryk, K. Hashimoto, A. Fujishima, Autoxidation of acetaldehyde initiated by TiO_2 photocatalysis under weak UV illumination, J. Phys. Chem. B102 (1998) 2699.
[34] J.L. Falconer, A. Kimberley, M. Bair, Photocatalytic and thermal catalytic oxidation of acetaldehyde on Pt/TiO_2, J. Catal. 179 (1998) 171.
[35] L. Yang, Z. Liu, J. Shi, Y. Zhang, H. Hu, W. Shangguan, Degradation of indoor gaseous formaldehyde by hybrid VUV and TiO_2/UV processes, Sep. Purif. Technol. 54 (2007) 204.
[36] S. Preis, A. Kachina, N.C. Santiago, J. Kallas, The dependence of temperature of gas-phase photocatalytic oxidation of methyl tert-butyl ether and tert-butyl alcohol, Catal. Today 101 (2005) 353.
[37] C. Guillard, B. Beaugiraud, C. Dutriez, J.-M. Herrmann, H. Jaffrezic, N. Jaffrezic-Renault, M. Lacroix, Physicochemical properties and photocatalytic activities of TiO_2-films prepared by sol–gel methods, Appl. Catal. B: Environ. 39 (2002) 331.
[38] Y. Chen, D.D. Dionysiou, A comparative study on physicochemical properties and photocatalytic behaviour of macroporous TiO_2-P25 composite films and macroporous TiO_2 films coated on stainless steel substrate, Appl. Catal. A: Gen. 317 (2007) 129–137.
[39] Y. Chen, D.D. Dionysiou, Effect of calcinations temperature on the photocatalytic activity and adhesion of TiO_2 films prepared by the P-25 powder-modified sol–gel method, J. Mol. Catal. A: Chem. 244 (2006) 73–82.
[40] M. Karches, M. Rudolf, P.L. von, J. Rohr, L. Giombi, M.A. Baltanas, Plasma CVD coated glass beads as photocatalyst for water decontamination, Catal. Today 72 (2002) 267.
[41] P. Davit, G. Martra, S. Coluccia, Photocatalytic degradation of organic compounds on TiO_2 powders-FT-IR investigation of surface reactivity and mechanistic aspects, J. Jpn. Petrol. Inst. 47 (2004) 359.
[42] A. Mills, G. Hill, M. Crow, S. Hodgen, Thick titania films for semiconductor photocatalysis, Rev. Appl. Electrochem. 35 (2005) 641.
[43] A. Fernandez, G. Lassaletta, V.M. Jimenez, A. Justo, A.R. Gonzalez-Elipe, J.-M. Herrmann, H. Tahiri, Y. Ait-Ichou, Preparation and characterization of TiO_2 photocatalysts supported on various rigid supports (glass, quartz and stainless steel). Comparative studies of photocatalytic activity in water purification, Appl. Catal. B: Environ. 7 (1995) 49.
[44] W. Choi, S.J. Hong, Y.-S. Chang, Y. Cho, Photocatalytic degradation of polychlorinated dibenzo-p-dioxins on TiO_2 film under UV or solar light irradiation, Environ. Sci. Technol. 34 (2000) 4810.